Implementation and evaluation of cloud analysis with WSR-88D reflectivity data for GSI and WRF-ARW

Ming Hu[1] and Ming Xue[1,2]

Received 21 November 2006; revised 4 February 2007; accepted 16 March 2007; published 13 April 2007.

[1] The cloud analysis procedure of the Advanced Regional Prediction System (ARPS) is implemented in a proposed operational numerical forecast system composed of the Grid-point Statistical Interpolation (GSI) and the Advanced Research WRF (WRF-ARW). The case of 23 May 2005 Central Plains storm cluster is used to assess the impact of the cloud analysis using reflectivity data from six operational WSR-88D radars within the proposed operational configuration on 6-h forecast of the storm cluster. The cloud analysis is shown to significantly reduce the spin-up problem and improve the short-range forecast for the storm cluster, even at the relatively coarse 9 km resolution. **Citation:** Hu, M., and M. Xue (2007), Implementation and evaluation of cloud analysis with WSR-88D reflectivity data for GSI and WRF-ARW, *Geophys. Res. Lett.*, *34*, L07808, doi:10.1029/2006GL028847.

1. Introduction

[2] The spin-up problem, which shows as the significant delay in the development of cloud and precipitation at the early stage of a model forecast, is a critical problem faced by the short-range forecast of high-impact weather. The spin-up problem is due to the absence or improper initialization of the cloud and precipitation systems and related mesoscale and storm-scale features in the initial condition and therefore can be mitigated through improving the analysis of such features, which at the storm-scale include in-cloud temperature, moisture, and hydrometeor disturbances. However, the hydrometeor fields are typically not analyzed in most analysis systems because of the lack of direct hydrometeor observations even though observations from, e.g., surface observation, satellite, and radar, do include information on cloud and precipitation. The spin-up problem is also responsible for NWP models' not being able to beat extrapolation-based nowcasting systems for very short-range precipitation forecasting [*Wilson et al.*, 1998].

[3] A semi-empirical complex cloud analysis procedure has been developed in recent years within the Advanced Regional Prediction System (ARPS) [*Xue et al.*, 2000; *Xue et al.*, 2001; *Xue et al.*, 2003] for analyzing cloud and hydrometeor fields and associated temperature and moisture disturbances using METAR, satellite, and radar observations. The ARPS cloud analysis had evolved from that of the Local Analysis and Prediction System (LAPS) [*Albers et al.*, 1996] with significant modifications documented by *Zhang* [1999] and *Brewster* [2002]. It was used with the WSR-88D data in several studies of tornadic thunderstorms at horizontal resolutions of 3 km or higher [*Xue et al.*, 2003; *Hu and Xue*, 2007; *Hu et al.*, 2006], and through frequent intermittent assimilation cycles. Those studies clearly showed that the cloud analysis procedure can effectively build up storms in the initial condition and therefore significantly reduce the spin-up problem.

[4] Encouraged by these results, we implemented the ARPS cloud analysis procedure within the National Centers for Environmental Prediction (NCEP) Grid-point Statistical Interpolation (GSI) [*Wu et al.*, 2002] framework, and examine the impact of the analysis of WSR-88D radar reflectivity data on the forecast of the Advanced Research WRF (WRF-ARW) [*Skamarock et al.*, 2005]. The GSI is being used to initialize the regional prediction models at NCEP and the WRF-ARW is a candidate for the next-generation Rapid Update Cycle (RUC), called the Rapid Refresh. Also, WRF-ARW is part of the multi-core short-range ensemble prediction system of NCEP.

[5] In this paper, the 23 May 2005 case of the Central Plains storm cluster is used to test the ARPS cloud analysis package in the above quasi-operational environment using a 9-km horizontal grid spacing, which is close to the resolution to be used for regional predictions at NCEP in the near future. In section 2, the 23 May 2005 case and the design of experiments are introduced. The results of experiments are analyzed in section 3 and summarized in section 4.

2. 23 May 2005 Case and Experimental Design

[6] At 0000 UTC 23 May 2005, a stationary front formed in the northern Oklahoma and the northern Arkansas and a storm-favorable environment with large CAPE and Storm Relative Helicity (SRH) was established near the Oklahoma-Kansas border. At 0300 UTC, two small storm cells were initiated north of the eastern Oklahoma-Kansas border and during the ensuing two hours more cells formed. By 0500 UTC, a NW-SE oriented storm cluster had formed from the southeastern Kansas to the southwestern Missouri. The cluster started to decay by 0900 UTC and became dissipated by 1300 UTC. It produced large hails and high winds over the Central Plains.

[7] The evolution of the cluster from 0600 to 1200 UTC, 13 March is illustrated in Figure 1, which shows the composite reflectivity fields observed by 6 WSR-88D radars around the cluster at 0600, 0900, and 1200 UTC. At 0600 UTC, the storm cluster was in its mature stage and included several strong cells distributed along the southeastern Kansas, northeastern Oklahoma, and southwestern

[1]Center for Analysis and Prediction of Storms, University of Oklahoma, Norman, Oklahoma, USA.
[2]School of Meteorology, University of Oklahoma, Norman, Oklahoma, USA.

0094-8276/07/2006GL028847$05.00

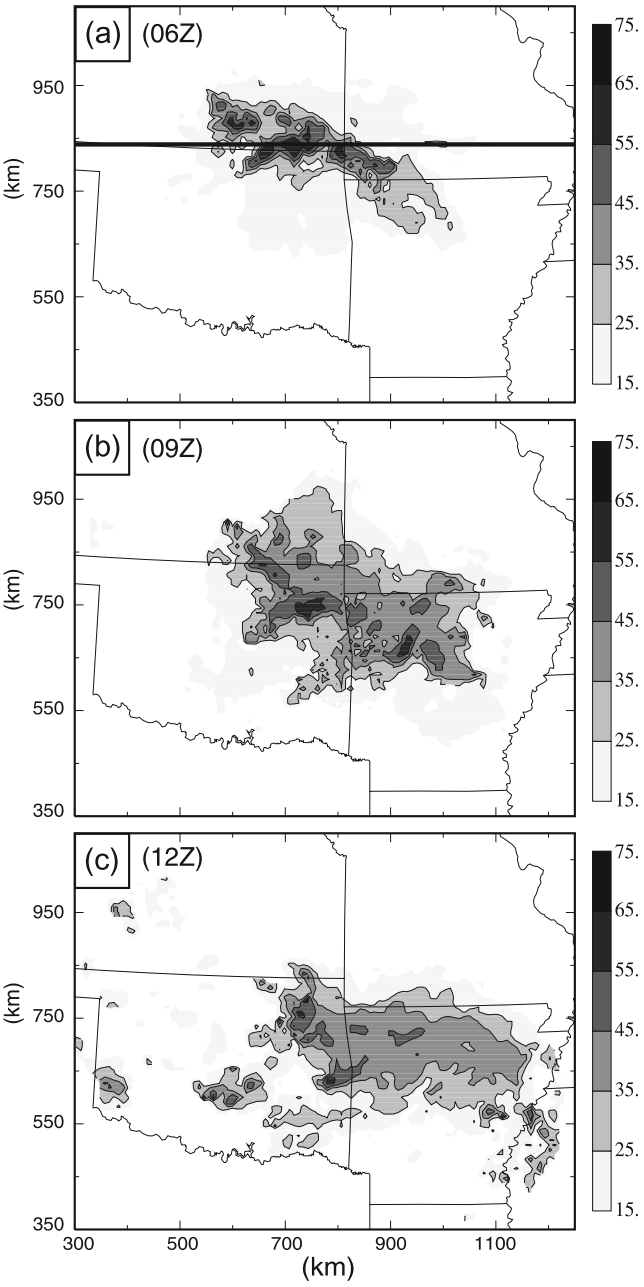

Figure 1. Composite reflectivity derived from reflectivity observations of KSRX (Fort Smith), KVNX (Vance Air Force Base), KTLX (Oklahoma City), KSGF (Springfield), KINX (Tulsa), and KLZK (Little Rock) radars at around 0600, 0900, and 1200 UTC, 23 May 2005. The domain shown represents the portion of the 9-km grid between 300 and 1250 km in the east-west direction and from 350 to 1050 km in the north-south direction.

Missouri (Figure 1a). The cluster moved southeastward in the next 6 hours. It sustained as a strong storm cluster until 0900 UTC (Figure 1b) but only had a few small cells left at the northeast of Oklahoma by 1200 UTC (Figure 1c).

[8] To study the impact of the ARPS cloud analysis on the storm forecast in the operational environment, the GSI analysis with conventional data (sounding, wind profiler, and surface observation) was performed at 0600 UTC, which serves as the background for the cloud analysis in the second pass. The details of the cloud analysis can be found in our previous paper [*Hu et al.*, 2006]. In this study, precipitation species are retrieved based on reflectivity equations from *Smith et al.* [1975] and in-cloud temperature is adjusted according to a moist adiabat originating from the cloud base. The WRF-ARW model using full model physics that includes land-surface model and *Lin et al.* [1983] ice microphysics but without cumulus parameterization was then run from the final analysis to predict the evolution of the storm cluster from 0600 to 1200 UTC. The simulation used a 9-km horizontal grid spacing and 30 vertical levels with the model top at about 50 hPa. The Lin scheme was used here because the ARPS cloud analysis has been mostly used together with the Lin scheme in the ARPS; the reflectivity formulas used in the cloud analysis are also consistent with the hydrometeor drop size distributions assumed by the Lin scheme. In this study, only radar observations at around 0600 UTC were used. Two experiments, one with the cloud analysis in the initial field (referred to CLD) and one without (referred to NoCLD), were conducted to isolate the effects of the cloud analysis. Otherwise, the two experiments are identical.

3. Results of Experiments

[9] The impacts of the radar data through the cloud analysis on the initial fields and the forecast of the storm cluster are analyzed in this section through the comparison of the two experiments and with radar reflectivity observations.

3.1. Impacts of Cloud Analysis on Initial Fields

[10] The ARPS cloud analysis procedure can add and remove hydrometeors and adjust in-cloud temperature and moisture in the analysis background fields. In this study, the cloud analysis was conducted at a relatively coarse 9-km grid spacing and its effects can be seen in terms of the analysis increments due to the cloud analysis. The east-west cross sections of the cloud analysis increments are plotted in Figure 2, together with the corresponding observed reflectivity field.

[11] At 0600 UTC, several storm cells were observed between x = 500 and 1000 km (Figure 2a) within the cross-section shown in Figure 2. The strongest storm was located at around x = 700 km which had an over-shooting top above the tropopause. Because reflectivity is the only observed quantity used in the cloud analysis in the current case, the analyzed hydrometeors are all distributed within the reflectivity area (the analysis with conventional data did not contain any hydrometeors). Vertically, cloud ice and snow are found from the middle to upper troposphere (Figures 2d and 2e), cloud water between 2 and 8 km levels (Figure 2c), and rain and hail in the lower troposphere only (Figures 2f and 2g). Horizontally, cloud water and rain are much broader in scale than cloud ice, snow because the latter are found at the upper levels where the reflectivity region is narrower (because additional shallower precipitation exists at the lower levels, Figures 2c–2g).

[12] To take into account of the latent heating in the updraft region, the cloud analysis adds positive temperature perturbations within the cloud and precipitation area based on the moist adiabat of an air parcel lifted from the low level

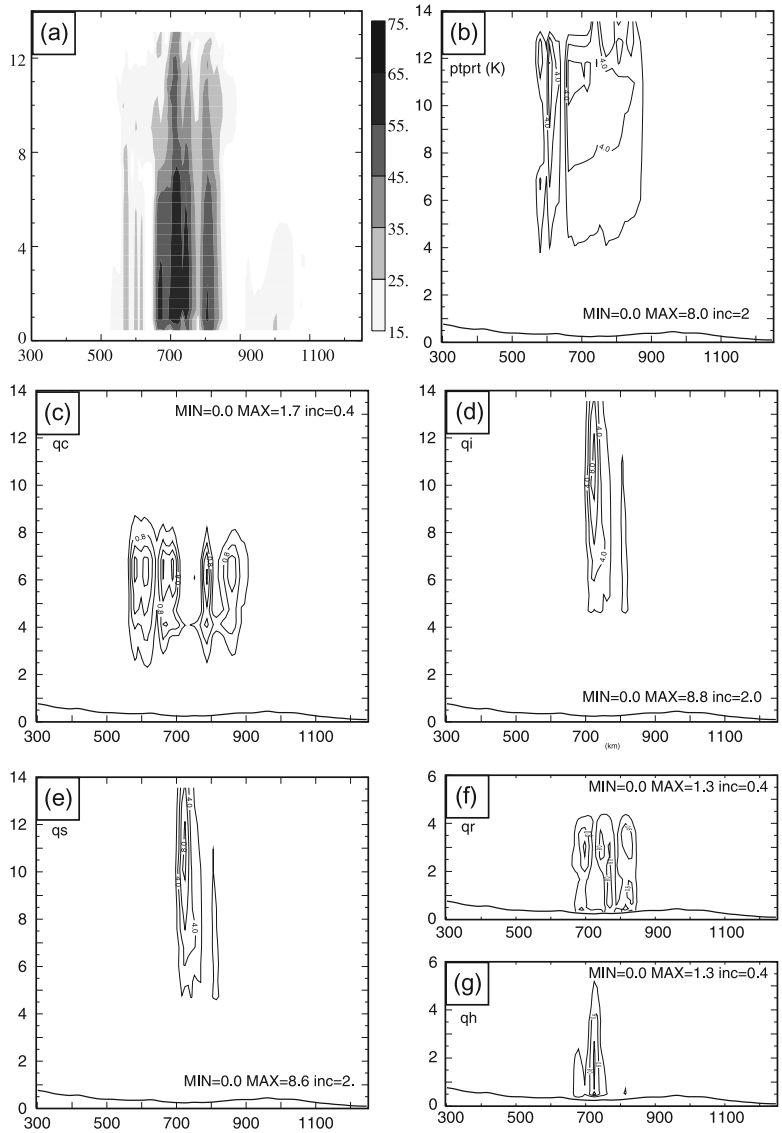

Figure 2. The x-z cross sections along the line shown in Figure 1a. (a) Observed reflectivity field in dBZ. (b) Cloud analysis increments of in-cloud temperature in K. (c) Cloud water q_c, (d) cloud ice q_i, (e) snow q_s, (f) rain q_r, and (g) hail q_h in g kg^{-1}. The x-coordinate is distance in km from the west boundary. The numbers are the maximum (MAX), minimum (MIN), and contour increment (inc).

[*Brewster*, 2002; *Hu et al.*, 2006]. This in-cloud temperature adjustment is shown as the temperature analysis increment in Figure 2b, where a maximum of 8 K adjustment is found at the upper levels, and most of the adjustment is found above 4 km. These positive temperature perturbations are important in offsetting the negative buoyancy associated with the introduction of hydrometeors and the associated evaporative cooling, and in sustaining existing storms and supporting possible development of the storms [*Hu et al.*, 2006; *Hu and Xue*, 2006].

3.2. Impacts of Cloud Analysis on Forecast of Storm Cluster

[13] Experiment CLD ran the WRF-ARW model for 6 hours starting from the initial fields in which the storm-related hydrometeor and temperature disturbances have been added by the cloud analysis. Experiment NoCLD differs from CLD in that the original GSI analysis is used as the initial condition without cloud analysis. The predicted composite reflectivity fields at 3 and 6 hours of forecast from these two experiments are plotted in Figure 3. To quantitatively compare the 6-hour-long forecasts of these two experiments, equitable threat scores (ETS) [*Schaefer*, 1990] of the predicted composite reflectivity for the 20 dBZ threshold are calculated against the observations and given in Table 1.

[14] When the reflectivity data are analyzed via the cloud analysis in CLD, the reflectivity field in the initial condition matches the observation rather well, giving a ETS of 0.758, while NoCLD has no precipitation at the initial time and therefore a ETS of 0 (Table 1). For the entire length of forecast, the ETS scores of CLD are much higher than those of NoCLD (Table 1), especially in the first two hours during which CLD predicts a cluster of strong storms moving slowly toward southeast as observed but NoCLD gives only

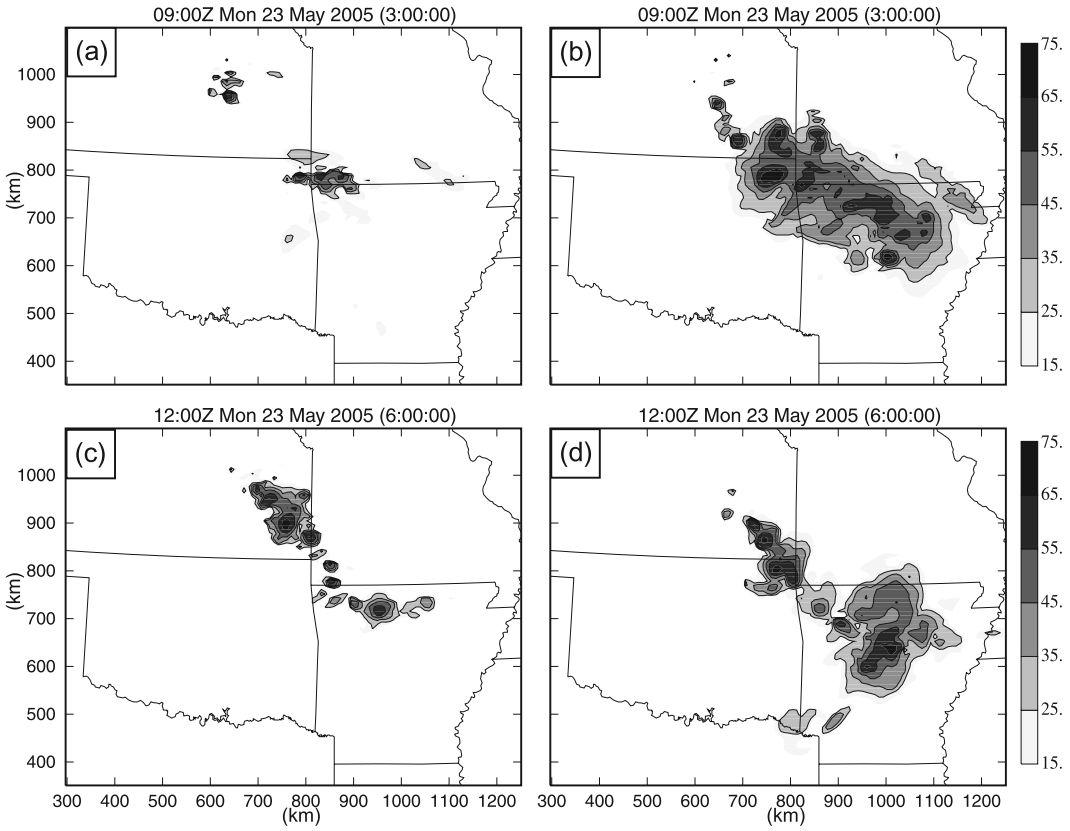

Figure 3. Composite reflectivity fields of 3 and 6 hour forecasts valid at (a, b) 0900 and (c, d) 1200 UTC, from experiments NoCLD (Figures 3a and 3c) and CLD (Figures 3b and 3d). The domain shown is the same as in Figure 1.

several weak echoes via gradual spin-up (not shown). The 3 and 6 hour forecasts of CLD predict a sustained storm cluster composed of several strong cells that propagates slowly southeastward (Figures 3b and 3d), while NoCLD only manages a few weak scattered cells at 3 hours and an elongated storm cluster of small cells at 6 hours (Figures 3a and 3c). The storm cluster predicted by NoCLD significantly lags behind the true storms in both time and space, due to a slow spin-up of the convection. With the help of cloud analysis, CLD captures the initial storms in its initial condition and is able to sustain the storms and predict the location and intensity of the observed storms well during the initial hours, although the observed transition into a weaker system at the later part of the forecast is handled less well.

[15] To look into more details of the forecast, the base-level reflectivity field of 5-h forecast valid at 1100 UTC from CLD and NoCLD is plotted in Figure 4, together with the corresponding observed reflectivity. Although the 5-h forecast misses most of the small cells observed by the radar, the forecast does capture the general intensity and shape of two main cells at this time (Figure 4), one at the southwest front and one at the northwest end of the storm cluster. Interestingly, both predicted and observed cells at the front of the cluster have elongated shape and an SW-NE orientation, which may have been due to the organization of outflow into a gust front. At this time, both predicted main cells have a northward displacement error of about 50 km. Between the above two cells, CLD also produces the third cell that can only be associated with a much weaker observed cell at a nearby location. Some of these discrepancies may be related to the relatively coarse horizontal resolution used here, which is too coarse to resolve smaller cells. Still, we can say that the 5-hour forecast of CLD captures main feathers of the individual cells in the storm cluster, and the forecast is much better than that of NoCLD at the same time (Figure 4c).

4. Summary and Discussion

[16] In this research, the ARPS cloud analysis procedure was implemented within a configuration that can potentially be implemented operationally. It consists of the NCEP GSI analysis system and the Advance Research version of the WRF prediction model. A case of storm cluster occurring in the Central Plains was used to assess the impacts of the cloud analysis using reflectivity data from six operational WSR-88D radars.

[17] In our previous studies [*Hu and Xue*, 2006; *Hu et al.*, 2006], the ARPS cloud analysis procedure was used within the ARPS analysis and forecast system at a 3-km horizontal

Table 1. Equitable Threat Scores of Predicted Composite Reflectivity for 20-dBZ Threshold

Forecast Hours	0	1	2	3	4	5	6
Experiment CLD	0.758	0.507	0.475	0.418	0.395	0.294	0.282
Experiment NoCld	0.000	0.066	0.138	0.057	0.042	0.042	0.042

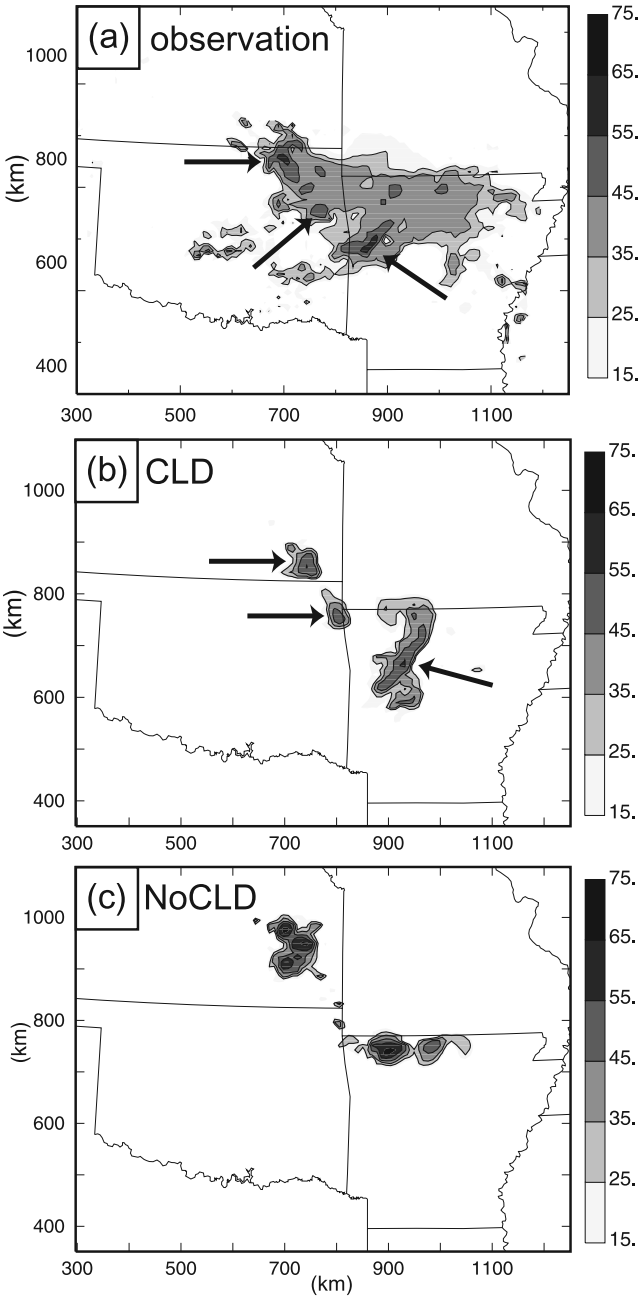

Figure 4. (a) Base-level radar reflectivity observation valid at 1100 UTC, and the corresponding 5-hour forecasts from experiments (b) CLD and (c) NoCLD. Arrows point to the main cells in Figure 4a and those captured by the forecast of CLD in Figure 4b.

grid spacing or higher. Focus there was on the initialization and prediction of individual storm cells. In this study, the impact of the cloud analysis is examined as using analysis and prediction systems of planned operational implementation at a resolution close to that of operational implementation at NCEP in the near future. The results clearly indicate that the cloud analysis with radar data significantly reduces the spin-up problem and can therefore improve the short-range (0–6 hours) forecast for precipitation systems similar to that studied here.

[18] The 9-km grid spacing examined falls within a gray area concerning the use of cumulus parameterization versus explicit microphysics. In our current case, explicit microphysics is used. One of the questions to ask is if the ARPS cloud analysis would work well at a 9 km resolution. The results of this study seem to suggest a positive answer. In our further study, CLD and NoCLD are repeated with both Kain-Fritsch [*Kain and Fritsch*, 1993] cumulus parameterization and explicit microphysics schemes turned on and the forecast results are found to be similar to their counterparts discussed in this paper. Currently, we are working on extending the ARPS cloud analysis package to better handle both convective and stratiform precipitations, to improve the use of satellite and ground-based cloud observations, and to implement the generalized cloud analysis package directly inside GSI. We will also examine the impact of the cloud analysis system on the forecast of the WRF-NMM core and in a more systematic manner and over extended periods. The WRF-NMM core is currently used in the operational North America Mesoscale (NAM) prediction system.

[19] **Acknowledgments.** This work was supported by DTC Visitor Program, and a DOT-FAA grant via DOC-NOAA NA17RJ1227. Xue was also supported by NSF grants ATM-0331756, ATM-0331594 and EEC-0313747. The GSI was provided by GSD of ESRL. Steve Weygandt and Shun Liu are thanked for very helpful discussions. GSD's high performance computing system was used for the experiments.

References

Albers, S. C., J. A. McGinley, D. A. Birkenheuer, and J. R. Smart (1996), The local analysis and prediction system (LAPS): Analysis of clouds, precipitation, and temperature, *Weather Forecasting*, *11*, 273–287.

Brewster, K. (2002), Recent advances in the diabatic initialization of a non-hydrostatic numerical model, paper presented at the 15th Conference on Numerical Weather Prediction and 21st Conference on Severe Local Storms, Am. Meteorol. Soc., San Antonio, Tex., 12–16 Aug.

Hu, M., and M. Xue (2007), Impact of configurations of rapid intermittent assimilation of WSR-88D radar data for the 8 May 2003 Oklahoma City tornadic thunderstorm case, *Mon. Weather Rev.*, *135*, 507–525.

Hu, M., M. Xue, and K. Brewster (2006), 3DVAR and cloud analysis with WSR-88D level-II data for the prediction of Fort Worth tornadic thunderstorms. part I: Cloud analysis and its impact, *Mon. Weather Rev.*, *134*, 675–698.

Kain, J. S., and J. M. Fritsch (1993), Convective parameterization for mesoscale models: The Kain-Fritsch scheme, *Meteorol. Monogr.*, *24*, 165–170.

Lin, Y.-L., R. D. Farley, and H. D. Orville (1983), Bulk parameterization of the snow field in a cloud model, *J. Clim. Appl. Meteorol.*, *22*, 1065–1092.

Schaefer, J. T. (1990), The critical success index as an indicator of warning skill, *Weather Forecasting*, *5*, 570–575.

Skamarock, W. C., J. B. Klemp, J. Dudhia, D. O. Gill, D. M. Barker, W. Wang, and J. D. Powers (2005), A description of the Advanced Research WRF Version 2, *NCAR Tech. Note 468+STR*, 88 pp., Boulder, Colo.

Smith, P. L., Jr., C. G. Myers, and H. D. Orville (1975), Radar reflectivity factor calculations in numerical cloud models using bulk parameterization of precipitation processes, *J. Appl. Meteorol.*, *14*, 1156–1165.

Wilson, J. W., N. A. Crook, C. K. Mueller, J. Sun, and M. Dixon (1998), Nowcasting thunderstorms: A status report, *Bull. Am. Meteorol. Soc.*, *79*, 2079–2099.

Wu, W.-S., R. J. Purser, and D. F. Parrish (2002), Three-dimensional variational analysis with spatially inhomogeneous covariances, *Mon. Weather Rev.*, *130*, 2905–2916.

Xue, M., K. K. Droegemeier, and V. Wong (2000), The Advanced Regional Prediction System (ARPS) – A multiscale nonhydrostatic atmospheric simulation and prediction tool. part I: Model dynamics and verification, *Meteorol. Atmos. Phys.*, *75*, 161–193.

Xue, M., K. K. Droegemeier, V. Wong, A. Shapiro, K. Brewster, F. Carr, D. Weber, Y. Liu, and D. Wang (2001), The Advanced Regional Predic-

tion System (ARPS) – A multi-scale nonhydrostatic atmospheric simulation and prediction tool. part II: Model physics and applications, *Meteorol. Atmos. Phys.*, *76*, 143–166.

Xue, M., D.-H. Wang, J.-D. Gao, K. Brewster, and K. K. Droegemeier (2003), The Advanced Regional Prediction System (ARPS), storm-scale numerical weather prediction and data assimilation, *Meteorol. Atmos. Phys.*, *82*, 139–170.

Zhang, J. (1999), Moisture and diabatic initialization based on radar and satellite observation, Ph.D. thesis, 194 pp., School of Meteorol., Univ. of Oklahoma, Norman, Okla.

M. Hu, Center for Analysis and Prediction of Storms, University of Oklahoma, Norman, OK 73072, USA.

M. Xue, School of Meteorology, University of Oklahoma, NWC Suite 2500, 120 David Boren Blvd, Norman, OK 73072, USA. (mxue@ou.edu)